Relative orientation of chemical shielding and dipolar coupling tensors: Mixed single- and double-quantum homonuclear rotary resonance nuclear magnetic resonance of rotating solids

M. Bak and N. C. Nielsen

Citation: The Journal of Chemical Physics **106**, 7587 (1997); doi: 10.1063/1.473761
View online: http://dx.doi.org/10.1063/1.473761
View Table of Contents: http://scitation.aip.org/content/aip/journal/jcp/106/18?ver=pdfcov
Published by the AIP Publishing

Relative orientation of chemical shielding and dipolar coupling tensors: Mixed single- and double-quantum homonuclear rotary resonance nuclear magnetic resonance of rotating solids

M. Bak and N. C. Nielsen
Department of Chemistry, University of Aarhus, DK-8000 Aarhus C, Denmark

(Received 3 July 1996; accepted 7 February 1997)

A novel two-dimensional magic-angle spinning nuclear magnetic resonance (NMR) method for determination of relative orientation of dipolar and chemical shielding tensors for dipolar-coupled homonuclear spin-1/2-pairs of powder samples is described. Simultaneous recoupling of anisotropic chemical shielding and dipolar coupling interactions is accomplished using a homonuclear rotary resonance pulse sequence with the amplitude ω_{rf} of a rf irradiation field matched to the spinning frequency ω_r according to $\omega_{\mathrm{rf}}=\omega_r$. Employing this technique in the first dimension of a two-dimensional experiment leads to powder spectra exhibiting strong dependence on the magnitudes and the relative orientation of the two shielding tensors and the dipolar coupling tensor correlated to a high-resolution spectrum in the sampling dimension. Various aspects of the recoupling experiment are described theoretically and the applicability of the method for determination of relative orientation of these three anisotropic tensors through numerical simulation is demonstrated on basis of experiments for a doubly ^{13}C-labeled powder of *L*-alanine. With reference to this sample (and aminoacids in general), minor effects from simultaneous recoupling of the heteronuclear dipolar coupling between C_α and the amide ^{14}N nucleus are evaluated. In the present case, the ^{13}C–^{14}N dipolar interaction is used in numerical simulations to refine our structural analysis and to obtain information about the absolute orientation of the ^{13}C chemical shielding tensors relative to the molecular coordinate system. © *1997 American Institute of Physics.* [S0021-9606(97)01618-8]

I. INTRODUCTION

The recent few years have witnessed a considerable interest in the development of solid-state nuclear magnetic resonance (NMR) methods capable of restoring weak dipole–dipole coupling interactions while employing magic-angle spinning (MAS) for obtaining high-resolution spectra.[1–11] These techniques have proven useful for determining internuclear distances,[1–7,12,13] chemical shift correlation,[7,8] and double-quantum (2Q) filtration[4,10,11,14] in a variety of polycrystalline solids. With the aim of obtaining dipolar recovery over a wide range of chemical shift differences and spectra depending exclusively on the structurally important dipolar couplings, these methods have to a great extent been developed specifically for dipolar recoupling while as efficiently as possible suppressing disturbing effects from chemical shielding. Nevertheless, several of the dipolar recoupling methods display minor effects from residual chemical shielding anisotropy (CSA) which may complicate straightforward extraction or exploitation of the dipolar couplings *but* may also be taken into advance to obtain structural information.[3,13,15,16] Even more useful in this regard would be methods specifically designed to efficiently recover both anisotropic chemical shielding and dipolar coupling interactions under high-resolution MAS conditions.

The magnitude and orientation of the chemical shielding tensor are known to be intimately related to the local electronic environment around the nuclei. Thus, valuable structural information may be obtained from such data either empirically based on compilations of shielding tensors from structurally well-characterized compounds,[17,18] by comparison with the results from *ab initio* calculations,[19] or if possible by combination with diffraction measurements.[20] For powder samples, the magnitudes of chemical shielding tensors may often be assessed using standard experiments. Generally, it is more complicated to obtain information about the orientation of these tensors relative to the molecular frame. Since the dipolar coupling interaction is uniquely oriented along the bonding axis, a versatile way to establish orientation information is to use methods *simultaneously* providing information about the anisotropic shielding and the dipolar coupling interactions. This information should optimally be achieved without losing the attractive features of high-resolution spectra. Therefore, development of dipolar recoupling MAS techniques providing high-resolution spectra of powder samples while simultaneously restoring a significant part of the CSAs may offer an attractive route to structural information which otherwise might be difficult to obtain. We note that alternative NMR methods capable of giving similar information and which involve single crystals,[21] static powders,[20,22] or samples rotating under off-MAS conditions[16,23] may be complicated either because single crystals can be difficult to produce or because of overlapping powder patterns in the spectral region from which the structural information has to be extracted.

A novel variant of the *ho*monuclear *ro*tary *r*esonance (HORROR) experiment[11] promises to serve a large part of the needs described above. By establishing the $\omega_r=\omega_{\mathrm{rf}}$ rotary resonance condition between the spinning frequency

ω_r and the amplitude $\omega_{\rm rf}$ of a rf irradiation field applied in the t_1 period of a 2D experiment, this method enables correlation of a simultaneously recovered dipolar coupling and CSA powder pattern in the first dimension of the 2D spectrum with a high-resolution MAS spectrum in the other dimension. Thus, while a previous study[11] focused on selective dipolar recoupling using double-quantum HORROR (2Q-HORROR) with $\omega_r = 2\omega_{\rm rf}$, this work examines the so-called *m*ixed *s*ingle-quantum and *d*ouble-quantum homonuclear rotary resonance (MSD-HORROR) experiment ($\omega_r = \omega_{\rm rf}$) *additionally* providing efficient recoupling of the CSAs. Specifically, the MSD-HORROR technique is analyzed as a means to determine relative orientation of the dipolar coupling tensor and the two anisotropic chemical shielding tensors of homonuclear dipole–dipole coupled spin-1/2-pair systems. The experiment is described theoretically in Sec. II. In Sec. IV the utility of the method for determination of relative orientation of ^{13}C–^{13}C dipolar and ^{13}C chemical shielding interaction tensors through numerical simulation and iterative fitting is demonstrated on basis of experiments for a doubly ^{13}C-labeled powder sample of *L*-alanine. Minor effects from heteronuclear dipolar coupling between C_α and the directly attached ^{14}N nucleus also being recoupled by rotary resonance is analyzed. The effect of the ^{13}C–^{14}N dipolar interaction is exploited to refine the relative orientation of the ^{13}C–^{13}C spin-pair tensors and relate these unambiguously to the molecular coordinate system. The results are discussed in relation to earlier data from x-ray diffraction,[24] neutron diffraction,[25] and single-crystal NMR (Ref. 26) studies.

II. THEORY

In this section we describe the theory necessary for understanding the MSD-HORROR recoupling phenomenon and for numerical simulation of the response of a homonuclear spin-1/2 pair to the general 2D HORROR pulse scheme in Fig. 1.

In its basic form [Fig. 1(a)], the pulse sequence consists of a soft x-phase rf pulse, with amplitude $\omega_{\rm rf} = -\gamma B_{\rm rf}$ matched to the sample rotation frequency ω_r according to the condition

$$\omega_r = n\omega_{\rm rf} \tag{1}$$

and bracketed by strong $\pi/2$ pulses of phases y and $-y$. The soft pulse is incremented during the t_1 period of the 2D experiment. As will be demonstrated in the following, fulfillment of Eq. (1) with $n = \pm 1$ (MSD-HORROR) or ± 2 (2Q-HORROR) ensures partial restoration of the nonsecular terms of the dipolar interaction under MAS conditions.[11] While effects from chemical shielding are efficiently suppressed in the 2Q-HORROR experiment, the MSD-HORROR experiment displays strong dependence on the anisotropic part of this interaction. In practice, as shown in Fig. 1(b), the initial $\pi/2$ pulse is often replaced by a cross-polarization (CP) sequence and the last $\pi/2$ pulse omitted to retain observable single-quantum coherences (1QCs).

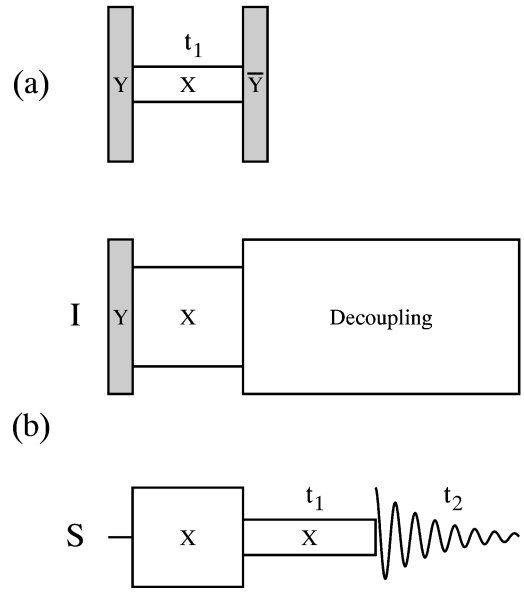

FIG. 1. Pulse schemes for homonuclear rotary resonance (HORROR) MAS experiments. Shaded bars represent $\pi/2$ pulses. (a) Basic 2D HORROR pulse sequence employed for the theoretical description. (b) Practically relevant 2D HORROR sequence combined with cross-polarization. The rf field strength in the t_1 period is ideally adjusted to $\omega_r = \omega_{\rm rf}$ for MSD-HORROR experiments (see text).

A. The spin-pair Hamiltonian of the HORROR experiment

In rotating solids, the high-field truncated Hamiltonian of a homonuclear $S_A - S_B$ spin-pair system influenced by chemical shielding, dipolar coupling, and scalar J coupling interactions as well as rf irradiation may be written

$$H(t) = \omega_A(t)T^A_{1,0} + \omega_B(t)T^B_{1,0} + \omega_D(t)T^D_{2,0} + \omega_J T^J_{0,0} + \omega_{\rm rf}(S_{Ax} + S_{Bx}). \tag{2}$$

The spin part of the internal Hamiltonian is described by irreducible spherical tensor operators[17] of which the following single-spin operators are relevant for the chemical shielding interaction ($\lambda = A$ or B):

$$T^\lambda_{1,0} = S_{\lambda z}, \quad T^\lambda_{1,\pm 1} = \mp\frac{1}{\sqrt{2}} S^\pm_\lambda \tag{3}$$

and the following spin-pair operators for the J (assumed isotropic) and dipolar (D) coupling interactions:

$$T^J_{0,0} = -\frac{1}{\sqrt{3}}\mathbf{S}_A\cdot\mathbf{S}_B, \quad T^D_{2,0} = \frac{1}{\sqrt{6}}(3S_{Az}S_{Bz} - \mathbf{S}_A\cdot\mathbf{S}_B),$$
$$T^D_{2,\pm 1} = \mp\frac{1}{2}(S^\pm_A S_{Bz} + S_{Az}S^\pm_B), \quad T^D_{2,\pm 2} = \frac{1}{2}S^\pm_A S^\pm_B. \tag{4}$$

The time and orientation dependence of the internal Hamiltonian is expressed through the coefficients

$$\omega_\lambda(t) = \sum_{m=-2}^{2} \omega^{(m)}_\lambda \exp(im\omega_r t), \tag{5}$$

where λ refers to the chemical shielding interaction of the two spins (A or B), the dipolar coupling (D), or the isotropic J coupling (J). $\omega_\lambda^{(m)}$ describes complex rotational Fourier components given by[3]

$$\omega_\lambda^{(m)} = \omega_{\rm iso}^\lambda \delta_{m=0} + \omega_{\rm aniso}^\lambda \Big\{ D^2_{0,-m}(\Omega^\lambda_{PR}) - \frac{\eta^\lambda}{\sqrt{6}} [D^2_{-2,-m}(\Omega^\lambda_{PR}) + D^2_{2,-m}(\Omega^\lambda_{PR})] \Big\} d^2_{-m,0}(\beta_{RL}), \tag{6}$$

where $\omega_{\rm iso}^\lambda = -\omega_0 \sigma_{\rm iso}^\lambda$ and $\omega_{\rm aniso}^\lambda = -\omega_0 \sigma_{\rm aniso}^\lambda$ for $\lambda = A$ or B, $\omega_{\rm iso}^J = -\sqrt{3}\pi J_{AB}$, and $\omega_{\rm aniso}^D = \sqrt{6} b_{AB} = -\sqrt{6}\mu_0 \gamma_A \gamma_B \hbar/(4\pi r_{AB}^3)$ ($\omega_{\rm aniso}^J = \omega_{\rm iso}^D = 0$). $\sigma_{\rm iso}^\lambda$, $\sigma_{\rm aniso}^\lambda$, J_{AB}, and b_{AB} denote the isotropic chemical shift, the chemical shielding anisotropy, the scalar J coupling, and the dipolar coupling, respectively (all in angular frequency units); r_{AB} is the internuclear distance. Among the anisotropic interactions only the CSA may exhibit a nonzero asymmetry parameter $0 \leqslant \eta^\lambda \leqslant 1$. The chemical shielding parameters are related to the principal values of the shielding tensor according to $\sigma_{\rm iso}^\lambda = \frac{1}{3}(\sigma_{xx}^\lambda + \sigma_{yy}^\lambda + \sigma_{zz}^\lambda)$, $\sigma_{\rm aniso}^\lambda = \sigma_{zz}^\lambda - \sigma_{\rm iso}^\lambda$, and $\eta^\lambda = (\sigma_{yy}^\lambda - \sigma_{xx}^\lambda)/(\sigma_{zz}^\lambda - \sigma_{\rm iso}^\lambda)$ using the ordering $|\sigma_{zz}^\lambda - \sigma_{\rm iso}^\lambda| \geqslant |\sigma_{xx}^\lambda - \sigma_{\rm iso}^\lambda| \geqslant |\sigma_{yy}^\lambda - \sigma_{\rm iso}^\lambda|$ (i.e., σ_{zz}^λ defined as the element being furthest away from $\sigma_{\rm iso}^\lambda$). $D^2_{p,q}(\Omega^\lambda_{PR})$ is an element of the second-rank Wigner matrix[27] describing transformation from the principal axis frame P^λ of the interaction λ through a given crystal-fixed frame C (in this work chosen coincident with P^D) to the rotor frame R, i.e.,

$$D^2_{p,q}(\Omega^\lambda_{PR}) = \sum_{k=-2}^{2} D^2_{p,k}(\Omega^\lambda_{PC}) D^2_{k,q}(\Omega_{CR}), \tag{7}$$

where $\Omega_{XY} = \{\alpha_{XY}, \beta_{XY}, \gamma_{XY}\}$ denotes the Euler angles relating the frames X and Y. We note that Ω^λ_{PC} specifies the desired orientation of the tensor for the interaction λ relative to the crystal-fixed frame. Ω_{CR} represents the so-called powder angles describing the orientation of the individual crystallite relative to rotor-fixed frame. Finally, the reduced Wigner function[17] $d^2_{-m,0}(-\beta_{RL})$ relates to transformation from R to the laboratory frame L with $\beta_{RL} = \tan^{-1}(\sqrt{2})$ for MAS experiments.

The recoupling effect of the MSD-HORROR experiment may conveniently be demonstrated by transforming the spin Hamiltonian to an interaction frame defined by the rf irradiation of the HORROR pulse sequence [Fig. 1(a)]. For simplicity, the description is initially moved to the tilted frame imposed by the bracketing $(\pi/2)_{\pm y}$ pulses where the Hamiltonian takes the form

$$H^T(t) = \exp\left[i \frac{\pi}{2} (S_{Ay} + S_{By}) \right] H(t) \exp\left[-i \frac{\pi}{2} (S_{Ay} + S_{By}) \right] = \sum_{\lambda,m,\mu} \omega_\lambda^{(m)} d^l_{\mu,0}\left(-\frac{\pi}{2} \right) \times \exp(im\omega_r t) T^\lambda_{l,\mu} + \omega_{\rm rf}(S_{Az} + S_{Bz}), \tag{8}$$

with l denoting the rank of the spin-part tensor ($l=0$ for isotropic J coupling, $l=1$ for chemical shielding, $l=2$ for dipolar coupling), $\mu = -l, \ldots, l$ the spin rotational component, and $m = -2, \ldots, 2$ the spatial rotational component.

In the tilted frame, the propagator for a coupled spin-pair system may be written

$$U^T(t,0) = U^T_{\rm rf}(t,0) \hat{T} \exp\left[-i \int_0^t \widetilde{H}^T(\tau) d\tau \right], \tag{9}$$

where $\hat{T}$ is the Dyson time-ordering superoperator and $U^T_{\rm rf}(t,0) = \exp[-i\omega_{\rm rf} t (S_{Az} + S_{Bz})]$ defines the transformation from the tilted frame to the interaction frame of the rotary resonance rf irradiation. In the latter frame, the Hamiltonian is given by

$$\widetilde{H}^T(t) = U_{\rm rf}^{T^\dagger}(t,0) H^T(t) U^T_{\rm rf}(t,0) = \sum_{\lambda,m,\mu} \omega_\lambda^{(m)} d^l_{\mu,0}\left(-\frac{\pi}{2} \right) \exp[i(\mu\omega_{\rm rf} + m\omega_r)t] T^\lambda_{l,\mu}, \tag{10}$$

which clearly demonstrates interference between the time modulation imposed by MAS on the spatial part of the internal Hamiltonian and the modulation imposed by the external rf irradiation on the spin part of the Hamiltonian.

Since $\widetilde{H}^T(t)$ is cyclic, approximate analytical insight into the spin dynamics may be obtained by taking the average of this Hamiltonian over one cycle period provided $\omega_{\rm rf}$ and ω_r exceeds the amplitude of the remaining interactions. This corresponds to the zeroth-order (time-independent) average Hamiltonian. It is immediately recognized that the integral nature of the spatial $-2 \leqslant m \leqslant 2$ and spin $-l \leqslant \mu \leqslant l$ rotational components implies that achievement of a time-independent part of the interaction frame Hamiltonian requires ω_r and $\omega_{\rm rf}$ being matched according to one of the conditions in Eq. (1). For 2Q-HORROR fulfilling $\omega_r = 2\omega_{\rm rf}$ ($n = 2$), the spin-space rotational components of the time-independent part of the Hamiltonian are matched according to $\mu = -2m$ resulting in the zeroth-order average Hamiltonian over two rotor periods,[11]

$$\tilde{\bar{H}}^{(0)}_{n=2} = \sqrt{\frac{3}{8}} [\omega_D^{(-1)} T^D_{2,2} + \omega_D^{(1)} T^D_{2,-2}] \tag{11}$$

which displays zero-order dependence on the dipolar interaction alone. In contrast, the MSD-HORROR experiment fulfilling $\omega_r = \omega_{\rm rf}$ ($n=1$) matches spin-space rotational components according to $\mu = -m$. This leads to the average Hamiltonian over one rotor period

$$\bar{\tilde{H}}^{(0)}_{n=1}=\sqrt{\frac{3}{8}}\,[\omega_D^{(-2)}T^D_{2,2}+\omega_D^{(2)}T^D_{2,-2}]+\frac{1}{\sqrt{2}}\,[\omega_A^{(-1)}T^A_{1,1}-\omega_A^{(1)}T^A_{1,-1}+\omega_B^{(-1)}T^B_{1,1}-\omega_B^{(1)}T^B_{1,-1}] \tag{12}$$

displaying dependence on both dipolar and anisotropic chemical shielding interactions. It is seen that recoupling of the anisotropic chemical shielding and dipolar coupling interactions is conducted through single- and double-quantum terms, respectively, of the interaction frame average Hamiltonian. This explains our acronym MSD-HORROR (*m*ixed single- and *d*ouble-quantum HORROR). Furthermore, it is evident that due to selection of the $\omega_D^{(\pm 2)}$ Fourier components the dipolar scaling factor for MSD-HORROR is lower by a factor of $\sqrt{2}$ relative to the 2Q-HORROR experiment selecting the $\omega_D^{(\pm 1)}$ components. We note that influences from the isotropic chemical shifts are suppressed to zero order because of the factor $d^l_{0,0}(-\pi/2)=0$ imposed by the bracketing $(\pi/2)_{\pm y}$ pulses.

Finally, we should note that in case of chemical shielding tensors exhibiting relatively small anisotropies the HORROR matching condition should fulfil

$$\omega_r=\frac{n}{2}\left[\sqrt{\omega_{\rm rf}^2+(\omega_{\rm iso}^A)^2}+\sqrt{\omega_{\rm rf}^2+(\omega_{\rm iso}^B)^2}\right], \tag{13}$$

which qualitatively takes into account larger effective field amplitudes induced by finite isotropic chemical shifts for the two spins.

B. Numerical simulation and iterative fitting

Numerically exact simulations of HORROR spectra for a homonuclear S_A-S_B spin-pair system are readily performed using the Hamiltonian in Eq. (2) along with the spin operators $S_{Ax}+S_{Bx}$ and $S_A^-+S_B^-$ for the initial and ''observable'' spin states, respectively. However, a more convenient picture of the spin dynamics during the t_1 evolution period of the 2D experiment in Fig. 1(a) emerges by transforming the description to the tilted frame induced by the bracketing $(\pi/2)_{\pm y}$ pulses. In this case both the initial and the ''observable'' spin states are given by $2S_z^{14}=S_{Az}+S_{Bz}$ and the t_1 evolution may be described by

$$s(t_1)=\overline{\mathrm{Tr}[2S_z^{14}U^T(t_1,0)2S_z^{14}U^{T^\dagger}(t_1,0)]}=\frac{1}{8\pi^2}\int_0^{2\pi}d\alpha_{CR}\int_0^{\pi}\sin(\beta_{CR})d\beta_{CR}\times\int_0^{2\pi}d\gamma_{CR}s(t_1;\Omega_{CR}) \tag{14}$$

after taking the average over all uniformly distributed crystallite orientations. The contribution from a single crystallite is given by

$$s(t_1;\Omega_{CR})=|\langle 1|U^T(t_1,0)|1\rangle|^2-|\langle 1|U^T(t_1,0)|4\rangle|^2-|\langle 4|U^T(t_1,0)|1\rangle|^2+|\langle 4|U^T(t_1,0)|4\rangle|^2 \tag{15}$$

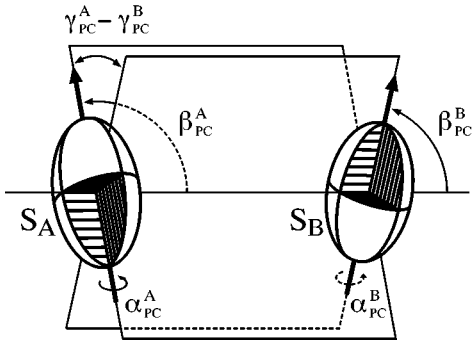

FIG. 2. Graphical definition of the Euler angles α^A_{PC}, β^A_{PC}, $\gamma^A_{PC}-\gamma^B_{PC}$, α^B_{PC}, and β^B_{PC} describing the orientation of the S_A- and S_B-spin chemical shielding tensors relative to the principal axis frame of the dipolar interaction. The dipolar coupling tensor is axially symmetric around the dipolar axis implying that the transverse dipolar components (not shown) may be chosen arbitrarily and thereby that no absolute values for γ^A_{PC} and γ^B_{PC} can be determined by analysis of the spin-pair alone (coupling to a third spin makes this possible, vide infra).

using the propagator

$$U^T(t_1,0)=\hat{T}\,\exp\left[-i\int_0^{t_1}H^T(t)dt\right] \tag{16}$$

with $H^T(t)$ defined by Eq. (8). It is seen that the evolution, as here written in the product $|m_A,m_B\rangle$ Zeeman eigenbase of the two-spin system, in the tilted frame is mapped purely in the 2Q subspace spanned by the two extreme Zeeman operators ($|1\rangle=|1/2,1/2\rangle$, $|4\rangle=|-1/2,-1/2\rangle$).

A simulation program, based on the above formulas and combined with nonlinear optimization routines, has been designed for iterative fitting to the experimental MSD-HORROR spectra in order to determine values for all (or some) of the 13 interaction parameters describing the magnitudes and relative orientation of the spin-pair chemical shielding, dipolar, and isotropic J coupling tensors in the principal axis frame of the dipolar interaction. Although all parameters ($\sigma^A_{\rm iso}$, $\sigma^A_{\rm aniso}$, η^A, $\sigma^B_{\rm iso}$, $\sigma^B_{\rm aniso}$, η^B, b_{AB}, J_{AB}, α^A_{PC}, β^A_{PC}, $\gamma^A_{PC}-\gamma^B_{PC}$, α^B_{PC}, and β^B_{PC}) in principle can be derived from the 2D MSD-HORROR spectra, the analysis performed in this work focuses on the Euler angles describing the relative orientations of the tensorial interactions. This effectively reduces the number of structural parameters to be fitted within the spin-pair analysis to five, which is fully legitimate in many cases of practical relevance. Parameters for the magnitudes of the involved interactions may typically be determined or estimated rather precisely by other means, e.g., using standard MAS and 2Q-HORROR experiments. We note that a version of the iterative fitting program also taking into account parameters involving additional heteronuclear dipolar coupling to a spin $I=1$ nucleus has been developed using similar principles (vide infra).

The orientations in terms of Euler angles of the two shielding tensors relative to the principal axis system of the dipolar interaction, specifically chosen coincident with the crystal-fixed frame C in this study, is defined in Fig. 2. It is noted that, since the dipolar tensor is axially symmetric, the choice of the transverse dipolar components (not indicated)

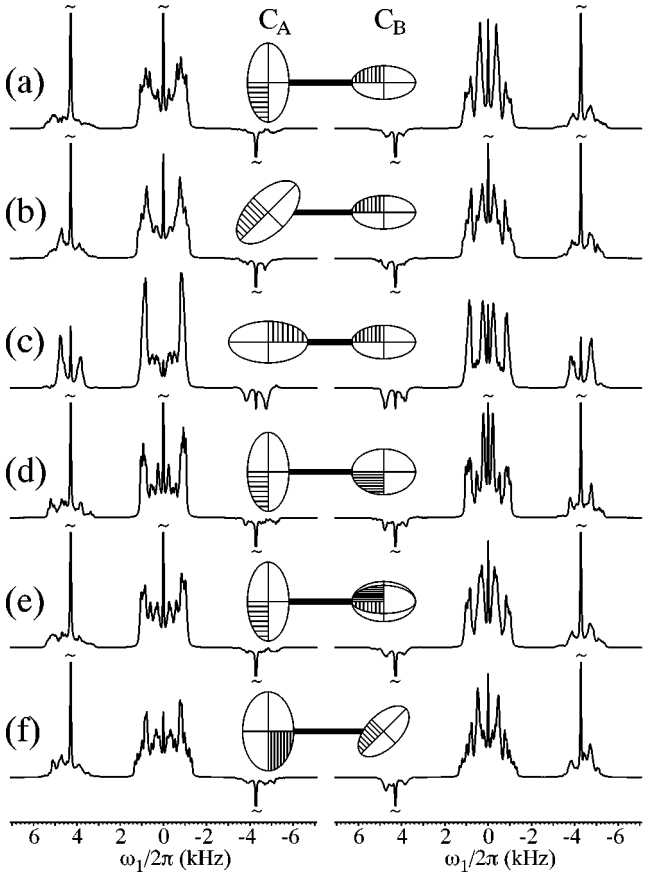

FIG. 3. Theoretical $\omega_1/2\pi$-dimension MSD-HORROR spectra calculated using tensor magnitudes corresponding to those of the C_AH-C_BH carbon spin-pair of *L*-alanine (at 100.6 MHz; parameters in Table I, $\omega_{rf}/2\pi=4000$ Hz, and $\omega_r/2\pi=4289$ Hz [according to Eq. (13)], and using different orientations of the two chemical shielding tensors relative to the dipolar coordinate system (visualized by ORTEP plots). Left and right column represent $\omega_1/2\pi$ projections for the C_A and C_B spins, respectively. The simulations employed $(\alpha_{PC}^A,\beta_{PC}^A,\gamma_{PC}^A)$ and $(\alpha_{PC}^B,\beta_{PC}^B,\gamma_{PC}^B)$ of (a) $(0,\pi/2,0)$ and $(0,0,0)$, (b) $(0,\pi/4,0)$ and $(0,0,0)$, (c) $(0,0,0)$ and $(0,0,0)$, (d) $(0,\pi/2,0)$ and $(0,0,\pi/2)$, (c) $(0,\pi/2,0)$ and $(0,0,\pi/4)$, and (f) $(\pi/2,\pi/2,0)$ and $(0,\pi/4,0)$.

is arbitrary implying that the spectra are invariant to an overall rotation of the tensors about the dipolar (internuclear) axis within the spin-pair approach. Thus, the absolute orientation of the spin-pair chemical shielding tensors in the molecular frame cannot be determined unambiguously from a MSD-HORROR powder spectrum unless interactions from other spins participate in the spin evolution (such as dipolar coupling to a heterospin as discussed in the following). Specifically, this limitation amounts to that it is possible to determine the torsion angle $\gamma_{PC}^A-\gamma_{PC}^B$ around the internuclear axis for the σ_{zz} principal shielding elements of the two spins but not individual values for γ_{PC}^A and γ_{PC}^B. In the process of determining the Euler angles, it is relevant to observe the following symmetry relations of the Fourier components:

$$\omega_\lambda^{(m)}(\alpha_{PC}^\lambda,\beta_{PC}^\lambda,\gamma_{PC}^\lambda)=\omega_\lambda^{(m)}(\pi+\alpha_{PC}^\lambda,\beta_{PC}^\lambda,\gamma_{PC}^\lambda)$$
$$=\omega_\lambda^{(m)}(\alpha_{PC}^\lambda,-\beta_{PC}^\lambda,\pi+\gamma_{PC}^\lambda), \qquad (17)$$

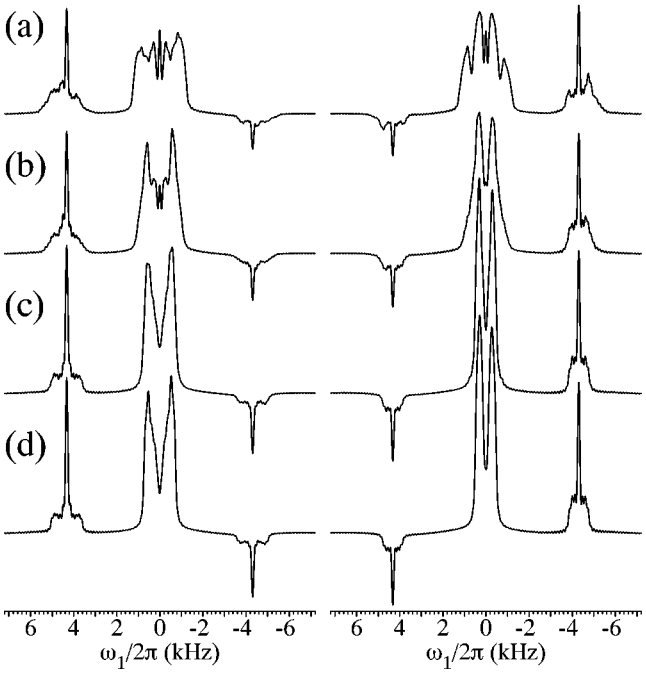

FIG. 4. Theoretical $\omega_1/2\pi$-dimension MSD-HORROR spectra calculated using $\omega_{rf}/2\pi=4021$ Hz, $\omega_r/2\pi=4313$ Hz, and tensor parameters corresponding to those of the $C_AH-C_BH_3$ carbon spin-pair of *L*-alanine (at 100.6 MHz; parameters in Table I) except for the dipolar coupling constant. Left and right column represent C_A and C_B, respectively. The simulations used dipolar coupling constants (internuclear distances in parentheses) of (a) 2224 Hz (1.5 Å), (b) 1401 Hz (1.75 Å), (c) 480 Hz (2.5 Å), and (d) 0 Hz (∞).

where the left-hand equation implies that α_{PC}^λ need only to be searched within a range of π.

To obtain accurate values for the various interaction parameters a simulation program based on the theory described above has been combined with the MINUIT least-squares optimization package[28] to allow iterative fitting of calculated to experimental $s(t_1)$ free induction decays. In the iterative fitting the chi-square deviation was defined as

$$\chi^2=kR=k\sum_{j=A,B}\sum_{n=1}^{N}|I_n^{\exp,j}-I_n^{\mathrm{sim},j}|^2, \qquad (18)$$

where R is the mean-squares difference between experimental and simulated intensities represented by the complex quantities $I_n^{\exp,j}$ and $I_n^{\mathrm{sim},j}$, respectively, for spin S_j and N is the number of points in the t_1 time domain signal. k is a scaling factor given by $(N-N_{\mathrm{par}})/R_{\min}$, where N_{par} is the number of fitted parameters and $R_{\min}$ is the minimum mean-squares difference. A well-defined value for the constant k is only relevant when using χ^2 for estimating accuracies for the fitted parameters in cases where the measurement errors (standard deviations) for the sample intensities are unknown but assumed equal for all sampling points.[29]

C. Sensitivity towards structural parameters and instrumental imperfections

To obtain an impression of the capability of MSD-HORROR as a means to achieve information about magni-

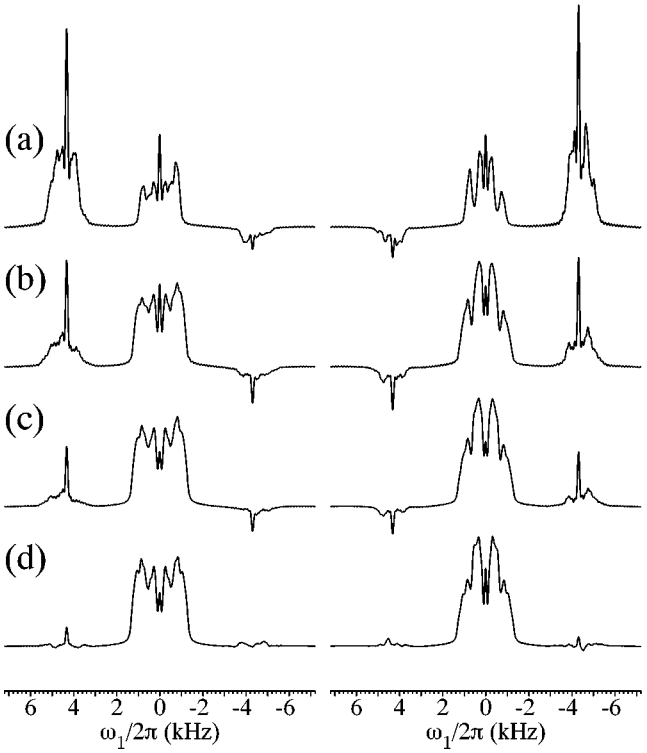

FIG. 5. Theoretical $\omega_1/2\pi$-dimension MSD-HORROR spectra calculated using parameters as in Fig. 4 except for $b_{AB}/2\pi = -2146$ Hz and the isotropic chemical shift difference $\omega^B_{\rm iso} - \omega^A_{\rm iso}$ being scaled by factors of (a) 2.0, (b) 1.0, (c) 0.5, and (d) 0.0.

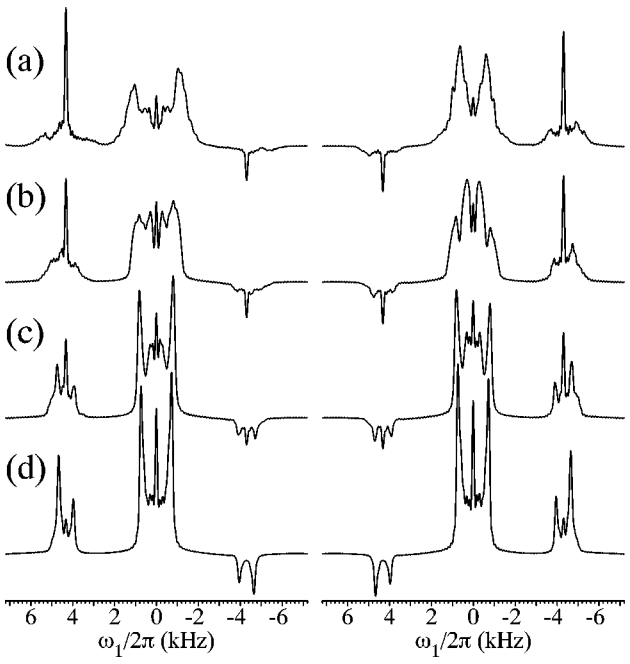

FIG. 6. Theoretical $\omega_1/2\pi$-dimension MSD-HORROR spectra calculated using parameters as in Fig. 4 except for $b_{AB}/2\pi = -2146$ Hz and the anisotropic chemical shifts $\omega^A_{\rm aniso}$ and $\omega^B_{\rm aniso}$ being scaled by factors of (a) 2.0, (b) 1.0, (c) 0.5, and (d) 0.0.

tudes and relative orientations of chemical shielding and dipolar coupling tensors in spin-1/2-pair systems, this section employs numerical simulations to investigate the impact of various parameters on the powder patterns observed for the two spins. To facilitate comparison with the results in the following section, all calculations are based on parameters for the $C_AH–C_BH_3$ carbon spin-pair system of *L*-alanine corresponding to experiments performed at a ^{13}C frequency of 100.6 MHz.

The dependence of the MSD-HORROR line shapes on the mutual orientation of two anisotropic chemical shielding tensors relative to the dipolar axis for a spin-1/2 pair in a powder sample is demonstrated in Fig. 3 by theoretical spectra using tensor magnitudes corresponding to C_AH and C_BH_3 in *L*-alanine. It is evident that the powder line shapes for both the C_A (largest CSA) and the C_B carbons depend markedly on the relative orientation of the three tensors indicated by ORTEP-like plots in Fig. 3 (the axially symmetric dipolar tensor is oriented along the bond axis). In particular, the powder patterns exhibit strong dependence upon variations of the β^A_{PC} and β^B_{PC} Euler angles in this case defining the direction of the most shielded chemical shielding tensor elements relative to the dipolar axis.

Obviously, the sensitivity of MSD-HORROR towards magnitudes and relative orientations of the three tensors depends on the relative magnitude of the various tensorial interactions as well as the rf field strength and the spinning frequency. The dependence on the dipolar coupling, which mediates the information about relative tensor orientations, is explored in Fig. 4. Clearly, upon increasing the internuclear distance from 1.5 Å corresponding to directly attached carbon spins up to infinity the MSD-HORROR spectrum gradually loses information about the dipolar coupling and thereby the relative tensor orientations. In the limit of vanishing dipolar coupling, the spectra provides information about the magnitudes of the chemical shielding tensors alone as recently investigated for the case of isolated spins by Gan *et al.*.[30]

For a typical one-bond $^{13}C–^{13}C$ dipolar coupling, variations in the isotropic shift difference [while maintaining the MSD-HORROR condition according to Eq. (13)] and in the magnitudes of the chemical shielding anisotropies are accompanied by significant spectral variations as illustrated in Figs. 5 and 6, respectively. Upon increasing the isotropic chemical shift difference the spectra gradually lose their symmetric/antisymmetric appearance and a significant part of the intensity is transferred from the centerband to one of the spinning sidebands. Likewise, a reduction of the CSAs gives rise to significant changes in powder line shapes and ultimately leads to spectra exhibiting strong dependence only on the homonuclear coupling interactions (the finite isotropic chemical shift difference introduces sidebands and a minor asymmetry in the individual S_A and S_B spectra). In the limit of vanishing CSAs the maximum splitting of the dipolar powder pattern corresponds well to the value of $3b_{AB}/4$ predicted by zero-order average Hamiltonian theory [Eq. (12)].

The effects associated with variation in the spinning speed, while maintaining $n=1$ rotary resonance according to Eq. (13), are explored in Fig. 7 by calculations using tenso-

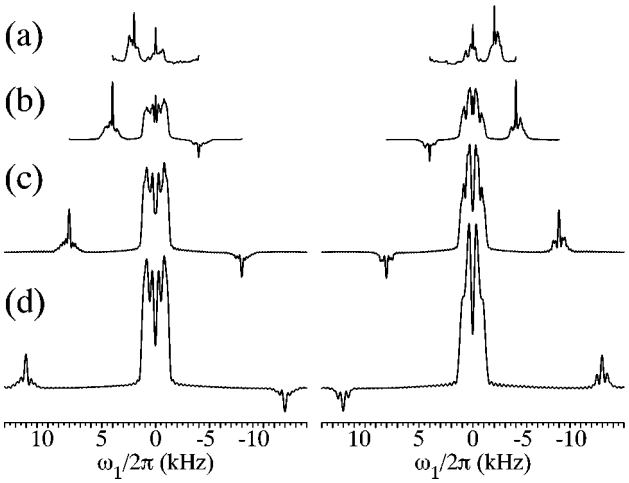

FIG. 7. Theoretical $\omega_1/2\pi$-dimension MSD-HORROR spectra calculated using parameters as in Fig. 4 except for $b_{AB}/2\pi = -2146$ Hz and MAS spinning frequencies of (a) 2, (b) 4, (c) 8, and (d) 12 kHz.

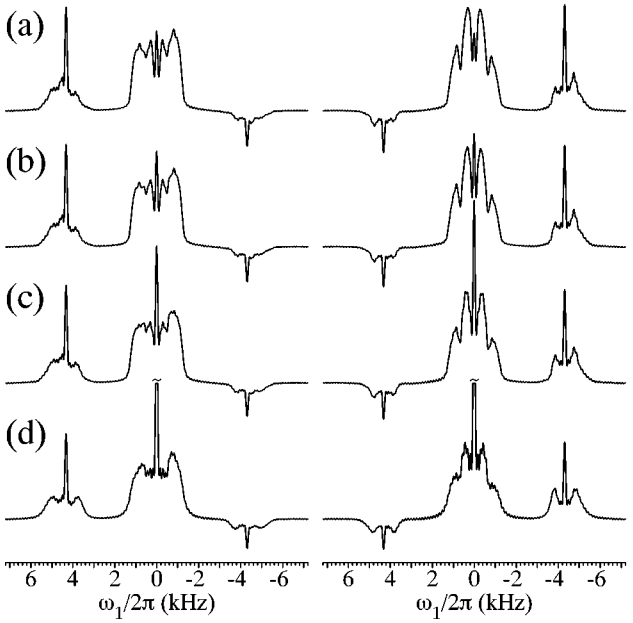

FIG. 8. Theoretical $\omega_1/2\pi$-dimension MSD-HORROR spectra calculated using parameters as in Fig. 7 except for $b_{AB}/2\pi = -2146$ Hz and a (a) 0 (0%), (b) 201 (5%), (c) 402 (10%), and (d) 804 (20%) Hz wide (FWHM) Gaussian distribution of the rf field strength centered around $\omega_{rf}/2\pi = 4021$ Hz.

rial parameters corresponding to the $C_A - C_B$ spin-pair of *L*-alanine. These simulations demonstrate that significant contributions to the line shapes from both chemical shielding and dipolar coupling interactions are obtained over a large span of spinning frequencies relative to the size of the anisotropic interactions. However, the spectra changes markedly upon increasing the spinning frequency which potentially may be taken into advantage to improve the accuracy of tensorial parameters extracted by numerical fitting of experimental spectra. For example, it is seen that the asymmetry of the spectra and the dominant sideband intensity gradually disappear for large spinning frequencies, while the powder pattern in the centerband preserves information about the anisotropic interactions even a high spinning frequencies.

Since the MSD-HORROR experiment relies on continuos rf irradiation throughout the t_1 period of the 2D experiment, it is of fundamental interest to examine its sensitivity towards inhomogeneity in the rf field. Rf inhomogeneity and instabilities in the MAS spinning frequency may cause to mismatch of the rotary resonance condition and thereby affect the spectral features of the powder patterns from which tensorial parameters have to be extracted. Figure 8 shows how MSD-HORROR spectra calculated for the $C_A - C_B$ spin-pair system of *L*-alanine using typical experimental conditions are affected by rf inhomogeneity. The spectra are calculated under the assumption of a Gaussian-shaped distribution of rf field strength with different widths covering inhomogeneities in the range of 0 to 20%. It appears that the technique is relatively robust towards rf inhomogeneity (and thereby also minor variations in the spinning speed) although excessive rf inhomogeneities should be avoided since they tend to smear out some of the most distinct spectral features.

D. Effects from $^{13}C_\alpha$–^{14}N dipolar coupling: Heteronuclear dipolar recoupling

With specific address to amino acids and other compounds having a ^{14}N nucleus attached to one of the ^{13}C–^{13}C spin-pair carbons, this section extends the above description to allow numerical analysis of the effects from ^{13}C–^{14}N dipolar coupling on the determination of parameters for the ^{13}C–^{13}C dipolar coupling and ^{13}C chemical shielding tensors. We note that various aspects of ^{13}C–^{14}N dipolar coupling and its influence on ^{13}C spectra have previously been discussed in detail by Stoll *et al.*[31] and by McDowell and co-workers.[26,32] In the present context, residual effects from ^{13}C–^{14}N dipolar coupling become particularly interesting because rf irradiation on the ^{13}C spins with a rf field strength matching the MSD-HORROR condition in Eq. (1) ($n = \pm 1$) also recouples the heteronuclear ^{13}C–^{14}N dipolar interaction.[6]

For amino acids, such as *L*-alanine, the ^{14}N (spin $I = 1$) quadrupolar coupling constant is typically in the order of 1–1.5 MHz. Using a strong magnetic field (such as 9.4 T, corresponding to a ^{14}N resonance frequency of 28.9 MHz), this interaction may to a good approximation be described by secular first-order terms being proportional to the irreducible tensor operator $T_{2,0}^{Q,N} = 3I_z^2 - \mathbf{I}(\mathbf{I}+1)$ with I referring to ^{14}N. Similarly, within the high-field approximation all heteronuclear dipolar $T_{2,m}^{D,CN}$ tensor components with $m \neq 0$ are truncated in the Zeeman interaction representation. Furthermore, the large heteronuclear chemical shift difference truncates all transverse components of $T_{2,0}^{D,CN}$. Under these favorable conditions, the ^{14}N quadrupolar coupling tensor become irrelevant for the ^{13}C spectrum since $T_{2,0}^{Q,N}$ and $2I_zS_{\lambda z}$ commutes. This represents an important simplification in the treatment of the ^{14}N heterospin but also opens up new aspects for structural investigation. With a known $^{13}C_\alpha$–^{14}N dipolar coupling constant, the orientation depen-

dent heteronuclear coupling may namely be exploited to unambiguously orient the ^{13}C chemical shielding tensors relative to a molecular coordinate system defined by the ^{13}C–^{13}C and $^{13}C_\alpha$–^{14}N bonding directions. Thus, in terms of parameters for the spin-pair system the additional $^{13}C_\alpha$–^{14}N interaction enables determination all six Euler angles describing the orientation of the shielding tensors in the crystal-fixed frame.

Within the high-field approximation, effects from the $^{13}C_A$–^{14}N dipolar coupling may be taken into account using

$$H_{\mathrm{CCN}}(t)=H_{\mathrm{CC}}(t)+\omega_{\mathrm{D,CN}}(t)2I_zS_{Az}, \tag{19}$$

where I and S refer to ^{14}N and ^{13}C, respectively. $H_{\mathrm{CC}}(t)$ represents the ^{13}C–^{13}C spin-pair Hamiltonian given by Eq. (2) and the heteronuclear dipolar coupling frequency $\omega_{\mathrm{D,CN}}(t)$ is defined in accordance to Eqs. (5) and (6). With respect to numerical simulations and iterative fitting, Eq. (19) have two immediate implications. First, the matrix representations increases from 4×4 to 12×12 leading to a significant reduction in the computation speed even in the most favourable block-diagonalizing representation. Second, the simulations need to take into account three additional parameters, namely the heteronuclear dipolar coupling constant $b_{\mathrm{CN}}/2\pi$ and the Euler angles $\Omega_{PC}^{\mathrm{CN}}=\{\alpha_{PC}^{\mathrm{CN}},\beta_{PC}^{\mathrm{CN}},0\}$ specifying the orientation of the C_A–N bonding axis relative to the ^{13}C chemical shielding and ^{13}C–^{13}C dipolar tensors.

III. EXPERIMENT

^{13}C MAS NMR spectra were recorded on a Varian Unity-400 spectrometer (9.4 T corresponding to a ^{13}C Larmor frequency of 100.6 MHz) equipped with a homebuilt MAS probe[33] and using 7 mm Si_3N_4 rotors. To reduce effects from rf inhomogeneity the rotors used an annulus shaped sample chamber (inner radius 3 mm, outer radius 5 mm, height 3 mm; 39 μl sample volume) of Kel–F to restrict the sample volume.[34] Using this setup, the rf field distribution is approximately of Gaussian shape with a half-width (FWHM) being about 5% of the nominal rf field amplitude. The experiments employed rf field strengths of 55, 40, and 4.16 kHz for ^1H pulses and decoupling, ^1H and ^{13}C spin-lock during CP and $^{13}C\pi/2$ pulses, and ^{13}C MSD-HORROR irradiation, respectively. The latter rf field strength was carefully calibrated under on-resonance conditions using the CH_3 resonance of 3-^{13}C-L-alanine. Prior to the experiment the magic angle was set within $\pm0.005°$ by minimizing the line width of the spinning sidebands for the $(\pm3/2,\pm1/2)$ satellite transitions in a ^{23}Na MAS spectrum of $NaNO_3$.[35] The spinning speed was stabilized within ±5 Hz using a Varian pneumatic spinning speed controller. ^{13}C chemical shift scales are in ppm relative to an external sample of tetramethylsilane (TMS). 99% doubly-enriched 2,3-$^{13}C_2$-L-alanine were purchased from Isotec, Inc. (Miamisburg, OH). Calculation of MSD-HORROR spectra were performed on a Digital Alpha 1000 4/200 workstation. Using a total of 232 crystallite orientations selected for $0\leqslant\alpha_{CR}\leqslant2\pi$ and $0\leqslant\beta_{CR}\leqslant\pi$ according to the scheme of Zaremba–Conroy–Wolfberg,[36] $0\leqslant\gamma_{CR}\leqslant2\pi$ averaging by time-translation of the Hamiltonian[2] (steps of 14.5 μs), 128 t_1 increments, and integration of the homogeneous evolution in steps of 4.8 μs, each spectrum required 23 s of CPU time. The CPU time increased by a factor 3 when including effects from the $^{13}C_\alpha$–^{14}N dipolar interaction.

IV. RESULTS AND DISCUSSION

In this section the capability of the MSD-HORROR technique for determining the orientation of anisotropic chemical shielding tensors in spin-1/2-pair systems relative to the internuclear axis is explored experimentally and numerically using a doubly-^{13}C-labeled sample of L-alanine. Specifically, the ^{13}C labels are incorporated on the $C_\alpha H$ and $C_\beta H_3$ carbons, henceforth referred to as C_A and C_B, respectively.

Doubly- or triply-^{13}C-enriched L-alanine has frequently been used as a model for a one-bond dipolar-coupled spin-pair system, for example, in the development of various dipolar recoupling solid-state NMR methods.[5,8,9,11,15] This may be ascribed to several facts: (i) amino acids in general are of great interest as structural units of peptides and proteins, (ii) ^{13}C-labeled crystals or powders of L-alanine are relatively easy to produce or commercially available, (iii) the structure has been determined using x-ray[24] and neutron diffraction,[25] and (iv) the magnitudes and orientations of the ^{13}C chemical shielding tensors relative to a molecular reference frame have been assessed using single-crystal NMR.[26] The diffraction studies indicate that the structure of L-alanine is orthorhombic (space group $P2_12_12_1$) with four molecules per unit cell which are mutually related by C_2 symmetry. The C_A–C_B intramolecular distance has been determined to 0.152 nm (Ref. 25) corresponding to a dipolar coupling of $b_{AB}/2\pi=-2146$ Hz which later has been confirmed by NMR.[8–10,15] Due to the relatively much larger intermolecular separation, the $^{13}C_AH$ and $^{13}C_BH_3$ carbons of the individual molecules may be regarded as isolated inequivalent spin pairs on the time scale of the MSD-HORROR experiment.

Since rf irradiation with amplitude $\omega_{\mathrm{rf}}=\omega_r$ on the ^{13}C spins also cause recoupling of the heteronuclear dipolar interactions involving ^{13}C, it is relevant also to consider effects from dipolar coupling between C_A and the directly attacted ^{14}N nucleus when examining L-alanine using the pulse sequence in Fig. 1. For several reasons, however, it appears convenient to separate the following treatment into a part considering the ^{13}C–^{13}C spin-pair alone followed by a part which *refines* data from the ^{13}C–^{13}C spin-pair analysis by additionally taking heteronuclear effects into account. First, the effects from the $^{13}C_A$–^{14}N dipolar coupling are typically relatively small compared to the relevant ^{13}C–^{13}C spin-pair interactions. Second, numerical calculations and iterative fitting considering both homo- and heteronuclear interactions for a ^{14}N–^{13}C–^{13}C three-spin system are considerably slower and involves more variables than ^{13}C–^{13}C spin-pair calculations. Third, a major object of the this paper is description of a technique for spin-pair analysis, implying that the second part can be left out of consideration for subsequent work not involving additional coupling to a heterospin.

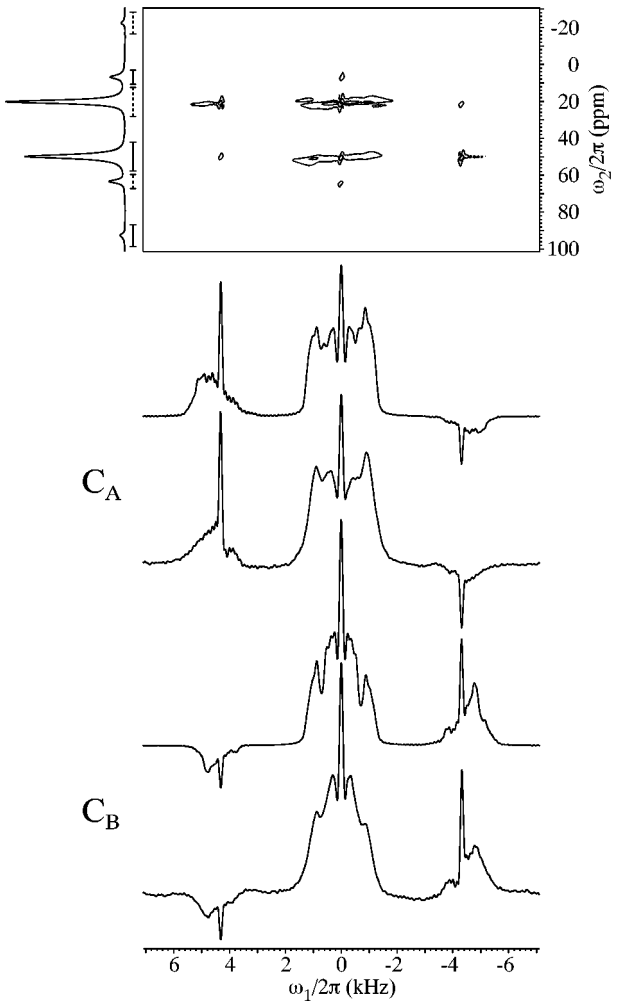

FIG. 9. Experimental and theoretical MSD-HORROR spectra of 2,3−$^{13}C_2$-*L*-alanine. (Top) Experimental 2D spectrum along with a projection onto the $\omega_2/2\pi$ (vertical) axis. (bottom) $\omega_1/2\pi$ projections through the indicated regions of the C_BH_3 (solid line) and C_AH (dashed line) resonances, respectively, of the experimental 2D spectrum. Above the experimental $\omega_1/2\pi$ projections are shown theoretical MSD-HORROR spectra for the C_BH_3 and C_AH resonances obtained using least-squares fitting to the experimental spectra within the ^{13}C–^{13}C spin-pair approach (i.e., neglecting dipolar coupling to ^{14}N). The optimum parameters corresponding to the theoretical spectra are given in Table I. The experimental 2D spectrum was obtained using the pulse sequence in Fig. 1 (b) with $\omega_r/2\pi = 4313$ Hz, $\omega_{rf}/2\pi$=4163 Hz (the latter value confirmed through iterative fitting), and 128 t_1 increments (4 transients each) separated by 58 μs. The rf carrier was on-resonance with respect to the mean isotropic chemical shift of the two spins.

TABLE I. Magnitudes and relative orientations for the C_AH and $C_BH_3{}^{13}C$ chemical shielding and C_A–C_B coupling tensors of 2,3 − $^{13}C_2$-*L*-alanine corresponding to the optimum simulations of the MSD-HORROR spectra in Figs. 9 and 12.[a]

	C_A	C_A–C_B	C_B
$\omega_{iso}/2\pi$[b]	−1558		1558
$\omega_{aniso}/2\pi$	1978		1177
η	0.44		0.76
σ_{xx}	−65.1		−30.3
σ_{yy}	−56.5		−21.4
σ_{zz}	−31.3		−8.3
α_{PC}	−48,[c] −40,[d] −36[e]		−43,[c] −96,[d] −50[e]
β_{PC}	108,[c] 99,[d] 90[e]		−11,[c] −17,[d] 4[e]
γ_{PC}	48,[c] 57,[d] 54[e]		0,[c] 76,[d] 0[e]
$b_{AB}/2\pi$		−2146	
J_{AB}		35	

[a]Euler angles are given in degrees. $\Omega_{PC}^{D,CC}=\{0,0,0\}$. Direct (dipolar) and indirect (J) coupling tensors are assumed axially symmetric and isotropic, respectively. Principal shielding elements are given in ppm relative to TMS while couplings as well as isotropic and anisotropic shifts are given in Hz ($\omega_0/2\pi=-100.6$ MHz). Magnitudes of dipolar coupling (internuclear distance) and chemical shielding tensors are taken from Refs. 25 and 26, respectively.

[b]Relative to the carrier frequency.

[c]Euler angles determined by analyzing the $^{13}C_A$–$^{13}C_B$ spin-pair without considering heteronuclear coupling to ^{14}N. Arbitrarily, we have chosen $\gamma_{PC}^B=0$ implying that $\gamma_{PC}^A=\gamma_{PC}^A-\gamma_{PC}^B$ represents the torsional angle around the internuclear axis.

[d]Refined Euler angles obtained by iterative fitting of the MSD-HORROR spectra taking into account the $^{13}C_A$–^{15}N dipolar interaction ($b_{C_AN}/2\pi=-665$ Hz, $\Omega_{PC}^{D,C_AN}=\{31°,70°,42°\}$).

[e]Euler angles determined by Naito *et al.* (Ref. 26) after correcting their tensors to conform with right-handed coordinate systems and transforming all tensors to the principal axis frame of the dipolar interaction.

A. The $^{13}C_A$–$^{13}C_B$ spin-pair of *L*-alanine

Because of relatively small CSAs and a small isotropic chemical shift difference (rendering rotational resonance experiments[1,3] impractical), the $^{13}C_A$–$^{13}C_B$ spin-pair of *L*-alanine may be regarded suitable for testing the applicability of the proposed method. Figure 9 shows a ^{13}C 2D MSD-HORROR spectrum for the ^{13}C–^{13}C two-spin system of powdered 2,3-$^{13}C_2$-*L*-alanine recorded using $\omega_r/2\pi = 4313$ Hz and $\omega_{rf}/2\pi$=4163 Hz grossly satisfying Eq. (13) when taking into account the actual isotropic chemical shift difference (rf irradiation on-resonance with respect to the mean isotropic chemical shift). The contour plot and the projection onto the vertical axis clearly reveal detection of a standard high-resolution MAS spectrum in the $\omega_2/2\pi$ dimension of the 2D experiment. It is noted that both ^{13}C resonances appear relatively narrow and featureless indicating that the ^{13}C–^{14}N dipolar coupling (C_A only) does not play a significant role in the $\omega_2/2\pi$ dimension under these experimental conditions. The powder patterns observed along the horizontal ($\omega_1/2\pi$) axis of the 2D spectrum and the projections through the C_AH and C_BH_3 resonances (regions indicated on the $\omega_2/2\pi$ axis of the contour plot) shown below the contour plot reflect the combined effects from anisotropic chemical shielding and dipolar coupling interactions active under MSD-HORROR conditions.

Using a dipolar coupling of $b_{AB}/2\pi=-2146$ Hz, an isotropic scalar coupling of $J_{AB}=35$ Hz (measured for dissolved *L*-alanine), and the magnitudes of the chemical shielding tensors issued by single-crystal NMR,[26] the experimental C_AH and C_BH_3 MSD-HORROR projections may be iteratively fitted to obtain values for the five Euler angles describing the orientation of the two ^{13}C shielding tensors relative to the principal axis frame of the ^{13}C–^{13}C dipolar coupling. In order to improve the reliability of the determined parameters, the fitting also involved the individual phases of the two t_1 free induction decays and the rf field strength. For the latter parameter, the optimum fit yielded a

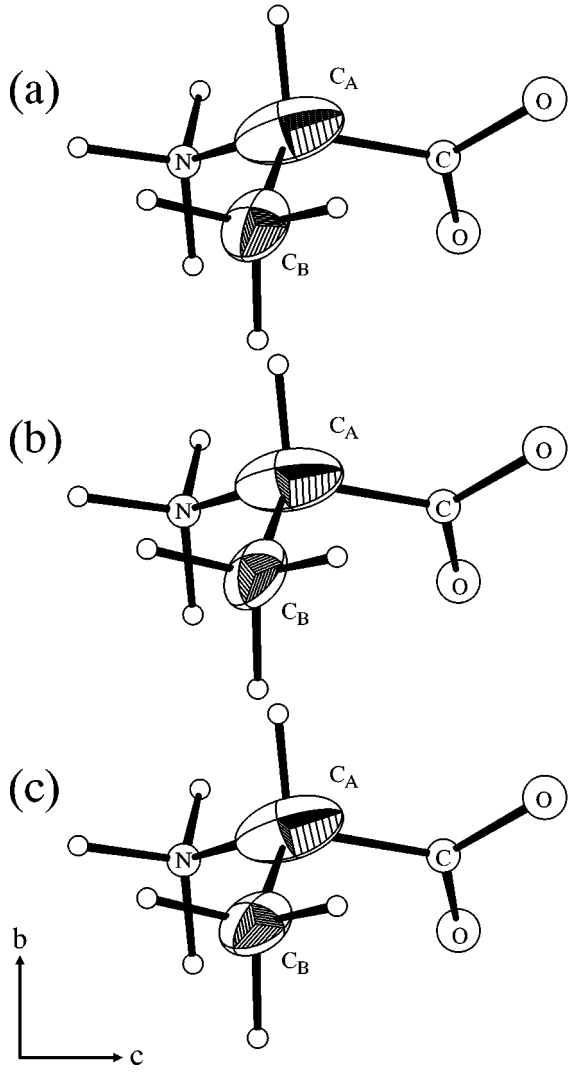

FIG. 10. ORTEP representations of the magnitudes and relative orientations of $^{13}C_AH$ and $^{13}C_BH_3$ carbon chemical shielding tensors determined using (a) MSD-HORROR without considering ^{13}C–^{14}N dipolar interactions, (b) single-crystal NMR (Ref. 26), and (c) MSD-HORROR upon refining the data from (a) by taking into account the $^{13}C_A$–^{14}N dipolar interaction. The length of the tensor ellipsoid axes are proportional to the principal values relative to a reference $\sigma_{\mathrm{ref}}=\sigma_{xx}-(\sigma_{zz}-\sigma_{xx})/0.9$ for the individual tensor (Ref. 17). The atomic positions are according to Ref. 25. The absolute orientation of the tensors with respect to rotation about the dipolar axis in (a) has arbitrarily been chosen similar to the a,b,c crystal-fixed frame of Naito *et al.* (Ref. 26).

value essentially identical to that found through calibration. The optimum Euler angles along with the magnitudes for the three tensorial interations are given in Table I. The simulated MSD-HORROR spectra corresponding to these parameters are included in Fig. 9 above the projections through the C_AH and C_BH_3 carbon resonances of the experimental spectrum.

A visualization of the magnitudes of the anisotropic shielding tensors and their orientation relative to the C_A–C_B bonding direction as determined by ^{13}C–^{13}C spin-pair analysis of the experimental MSD-HORROR spectrum is given in Fig. 10(a) by an ORTEP drawing. To relate the tensors to the molecular frame of *L*-alanine, the ORTEP plot used atomic coordinates taken from the neutron diffraction study of Lehman *et al.*[25] Since the overall rotation of the tensors about the internuclear axis remain undetermined by the ^{13}C–^{13}C spin-pair analysis all tensors were arbitrarily rotated about this axis to visually match the overall orientation determined by single-crystal NMR.[26] To facilitate direct comparison, Fig. 10(b) includes an ORTEP plot corresponding to the tensor orientations determined in a single-crystal NMR study by Naito *et al.*[25] after correction of their principal axis frame for the C_BH_3 shielding tensor to conform with a right-handed coordinate system (corresponding to replacement of β_{PC}^B with $\pi-\beta_{PC}^B$). Furthermore, the Euler angles from the single-crystal study are reproduced in Table I upon transformation of all tensors to the principal axis frame of the dipolar interaction. We note that the inconsistency in the methyl group tensor values of Naito *et al.*[26] has earlier been pointed out by Zhu *et al.*[37]

From the Euler angles determined by iterative fitting of the MSD-HORROR spectrum under the assumption of vanishing heteronuclear dipolar interactions, it is observed that the most shielded element of the methyl tensor is aligned close to the internuclear C_A–C_B axis (deviation by 11°) and thereby the threefold C_3 symmetry axis of the methyl group. Furthermore, the most shielded axis of the C_AH carbon shielding tensor is determined to be nearly perpendicular to this axis. These observations conform quantitatively well with the observations of Naito *et al.*[26] and with empirical rules for sp_3 hybridized carbons.[17,18] A similar agreement is observed for the α_{PC}^{λ} and γ_{PC}^{λ} Euler angles. A closer inspection of the direction corresponding to the Euler angles determined by single-crystal NMR (Ref. 26) and MSD-HORROR on a powder sample reveals that the orientation of all principal axes angles for the C_A and C_B shielding tensors agree within 22° and 17°, respectively. Taking into account the absolute uncertainties of the two measurements (including neglection of the $^{13}C_A$–^{14}N dipolar interaction, see next section) this appears to represent a rather favorable consistency of data.

In order to obtain a specific impression of the sensitivity (and thereby the accuracy) of MSD-HORROR towards the chemical shielding tensor orientations for *L*-alanine and its susceptibility towards local minimas in the iterative fitting, Fig. 11 shows plots of χ^2 as a function of the five Euler angle variables (cf. the definition in Fig. 2). From these plots it becomes apparent that MSD-HORROR is quite sensitive towards variations in β_{PC}^A and β_{PC}^B, specifying angles between internuclear axis and the largest shielding elements (σ_{zz}^{λ}) of the S_A (C_AH) and S_B(C_BH_3) spins, respectively. Slightly lower sensitivity is observed towards variations in α_{PC}^A and α_{PC}^B specifying the orientation of the two perpendicular elements of the C_A and C_B shielding tensors with respect to the internuclear axis. Likewise, a lower sensitivity is observed with respect to variation in the differential angle $\gamma_{PC}^A-\gamma_{PC}^B$ describing the torsion around the C_A–C_B internuclear axis for the largest principal shielding elements of the two spins. This interpretation conforms well with the variations in the MSD-HORROR powder line shapes observed for the various different tensor orientations in Fig. 3. It should

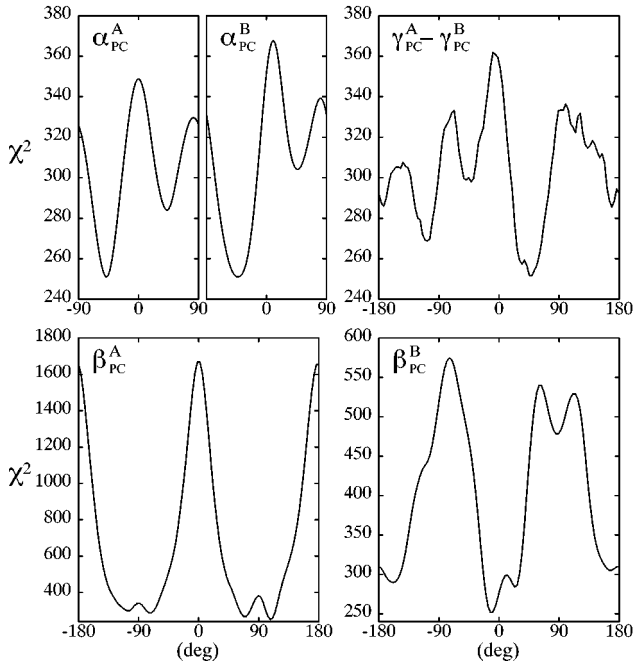

FIG. 11. Chi-square (χ^2) deviation between experimental and simulated MSD-HORROR spectra of 2,3$-{}^{13}C_2$-*L*-alanine plotted as function of α^A_{PC}, β^A_{PC}, α^B_{PC}, β^B_{PC}, and $\gamma^A_{PC}-\gamma^B_{PC}$. For all plots, the analysis are performed within ^{13}C–^{13}C spin-pair approach (neglecting heteronuclear dipolar interactions) and all except for the variable parameter take the values given for this approach in Table I.

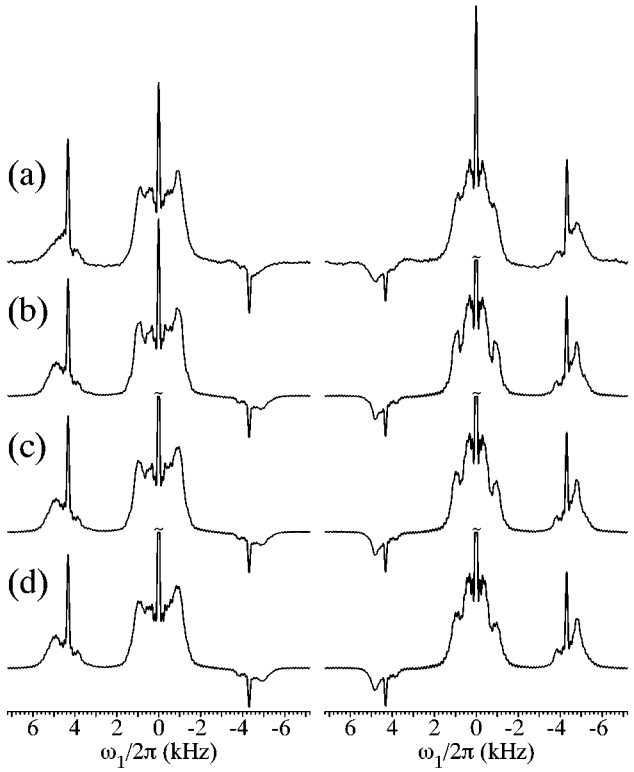

FIG. 12. Comparison experimental (a) and optimum simulated (b) $\omega_1/2\pi$-dimension MSD-HORROR spectra for the (right) C_BH_3 and (left) C_AH spins of *L*-alanine. The experimental spectra are taken from Fig. 9. The simulated spectra were obtained by iterative fitting to the experimental spectra while taking into account the ^{13}C–^{13}C spin-pair interactions as well as the $^{13}C_A$–^{14}N heteronuclear dipolar interaction. The iterative fitting, involving the six Euler angles specifying the shielding tensor orientations, used the results corresponding to the simulations in Fig. 9 as initial parameters and a magnitude and orientation of heteronuclear dipolar coupling corresponding to the geometry determined by neutron diffraction (Ref. 25). (c),(d) Theoretical spectra using the same parameters as in (b) but including (c) 5% and (d) 10% rf inhomogeneity (FWHM, Gaussian shape).

be noticed, however, that only crude estimations of the accuracies for the individual Euler angles may be obtained from the plots in Fig. 10 since they represents only one-dimensional traces through a five-dimensional parameter space. Furthermore, the sensitivity towards variation in the tensor orientations generally depends on the relative magnitudes of the chemical shielding and dipolar coupling tensors and therefore remain specific for this analysis.

B. Refinement taking into account the $^{13}C_A$–^{14}N dipolar interaction

Based on the results achieved by iterative fitting of the experimental MSD-HORROR spectrum of *L*-alanine within the numerically fast ^{13}C–^{13}C spin-pair approach, it is now feasible to additionally include the $^{13}C_A-{}^{14}N$ dipolar interaction in the calculations to obtain refined spectral parameters and further structural information. For this purpose the Hamiltonian in Eq. (19) is employed along with a heteronuclear dipolar coupling constant of $b_{C,N}/2\pi=-665$ Hz (corresponding to an internuclear distance of 1.486 Å) and the dipolar tensor oriented along the C_A-N bond direction according to the atomic coordinates of Lehman *et al.*[25] (cf. Fig. 10). Furthermore, the Euler angles determined above within the isolated ^{13}C–^{13}C spin-pair approach have been taken as a good initial estimate on the shielding tensor orientations relative to the C_A-C_B axis. Under these conditions, iterative fitting of the experimental MSD-HORROR spectrum with respect to the six Euler angles specifying the orientations of the two ^{13}C chemical shielding tensors leads to the refined parameters included Table I and the optimum simulated spectra in Fig. 12. For convenience, Fig. 10(c) includes the corresponding optimum chemical shielding tensor orientations visualized by ORTEP plots. Since it is known, that the experimental spectra are influenced by rf inhomogeneity in order of 5%, Fig. 12 also includes simulations taking into account 5% and 10% rf inhomogeneity. Clearly, rf inhomogeneity may account for part of the residual discrepancies between the experimental and optimum simulated MSD-HORROR spectra.

By comparing, the overall quality of the optimum simulated spectra in Fig. 12 with the corresponding spectra in Fig. 10, it is evident that the $^{13}C_A-{}^{14}N$ dipolar coupling recoupled by MSD-HORROR is responsible for spectral features which can not be simulated within the ^{13}C–^{13}C spin-pair approach alone. On the basis of iterative fitting, it can be concluded that consideration of the $^{13}C_A-{}^{14}N$ dipolar interaction not only improves the agreement between experimental and simulated spectra but also enables unambiguous orientation of the shielding tensors to a molecular frame specified by the ^{13}C–^{13}C and $^{13}C_A-{}^{14}N$ bonding axes. On the

other hand, by calculating the angles between the shielding tensor principal axes issued by the two calculations or comparing the ORTEP plots in Figs. 10(a) and 10(c), it can also be concluded that a rather good estimate on the relative tensor orientations may be obtained by iterative fitting without considering the heteronuclear coupling. Specifically, the principal axes agree within 14° and 15° for the C_A and C_B shielding tensors, respectively. The corresponding numbers obtained by comparison of principal axis orientations corresponding to the optimum fit in Fig. 12 and the single-crystal NMR study[26] is 10° and 30°. Clearly, the absolute orientations of the C_A shielding tensor agree within the experimental uncertainty for the two measurements. For the methyl tensor, the more unfavorable discrepancy is largely caused by a rotation of the tensor around the σ_{zz}^{B} axis (see Fig. 10). Apart from standard absolute uncertainties in the two measurements, being increased by the small anisotropy, this deviation may be influenced by external factors such as rf inhomogeneity and molecular dynamics. In this context, it seems appropriate to mention that 95% confidence intervals for the shielding tensor Euler angles, estimated on basis of the iterative fitting, indicate relative uncertainties of about $\pm 10°$ for α_{PC}^{λ} and γ_{PC}^{λ} and about $\pm 6°$ for β_{PC}^{λ} ($\lambda = A$ or B).

V. CONCLUSION

In summary, we have shown that MSD-HORROR represents a useful technique for determining magnitudes and relative orientation of chemical shielding and dipolar coupling tensors for spin-pair systems in powder samples. The method combines high-resolution MAS NMR in one dimension with anisotropic powder spectra in the other dimension from which information about magnitudes and relative orientation may be derived using numerical simulation and iterative fitting. Demonstration of the method for a doubly-^{13}C-enriched sample of *L*-alanine and comparison with the results from an earlier single-crystal NMR study shows that fairly accurate values for all tensor orientations may be determined from powder samples using the MSD-HORROR technique. It has been demonstrated that MSD-HORROR simulateneously recouples dipolar and chemical shielding interactions for the homonuclear $^{13}C-^{13}C$ spin-pair system and dipolar coupling for the heteronuclear $^{13}C-^{14}N$ spin-pair system. This effect has been exploited in $^{13}C-^{13}C-^{14}N$ three-spin calculations to obtain refined values for the ^{13}C chemical shielding tensors and their absolute orientations relative to the molecular frame.

Application of the MSD-HORROR technique and variants of this to other $^{13}C-^{13}C$ and $^{31}P-^{31}P$ spin pairs is currently being pursued in our laboratory as a more general means to obtain accurate values for tensor orientations. We expect the MSD-HORROR method to find its primary use for structural studies of amorphous and polycrystalline solids which cannot be crystallized easily (e.g., membrane proteins) and thereby not amenable to single-crystal NMR studies.

ACKNOWLEDGMENTS

The use of the facilities at the University of Aarhus NMR Laboratory, sponsored by Teknologistyrelsen, the Danish Research Councils (SNF and STVF), Carlsbergfondet and Direktor Ib Henriksens Fond, is acknowledged. We thank Aarhus University Research Foundation for equipment grants. The authors thank M. H. Levitt, M. Hohwy, H. Bildsøe, and H. J. Jakobsen for discussions and technical support.

[1] D. P. Raleigh, M. H. Levitt, and R. G. Griffin, Chem. Phys. Lett. **146**, 71 (1988); M. G. Colombo, B. H. Meier, and R. R. Ernst, *ibid.* **146**, 189 (1988); N. C. Nielsen, F. Creuzet, and R. G. Griffin, J. Magn. Reson. A **103**, 245 (1993).
[2] T. Gullion and J. Schaefer, J. Magn. Reson. **81**, 196 (1989); Y. Pan, T. Gullion, and J. Schaefer, *ibid.* **90**, 330 (1990); O. Weintraub, S. Vega, C. Hoelger, and H. H. Limbach, *ibid.* **109**, 14 (1994); M. Baldus, M. Tomaselli, B. H. Meier, and R. R. Ernst, Chem. Phys. Lett. **230**, 329 (1994); D. M. Gregory, D. J. Mitchell, J. A. Stringer, S. Kiihne, J. C. Shiels, J. Callahan, M. A. Mehta, and G. P. Drobny, *ibid.* **246**, 654 (1995).
[3] M. H. Levitt, D. P. Raleigh, F. Creuzet, and R. G. Griffin, J. Chem. Phys. **92**, 6347 (1990).
[4] R. Tycko and G. Dabbagh, Chem. Phys. Lett. **173**, 461 (1990); J. Am. Chem. Soc. **113**, 9444 (1991).
[5] T. Gullion and S. Vega, Chem. Phys. Lett. **194**, 423 (1992).
[6] T. G. Oas, R. G. Griffin, and M. H. Levitt, J. Chem. Phys. **89**, 692 (1988); M. H. Levitt, T. G. Oas, and R. G. Griffin, Isr. J. Chem. **28**, 271 (1988).
[7] B.-Q. Sun, P. R. Costa, D. Kocisko, P. T. Lansbury, Jr., and R. G. Griffin, J. Chem. Phys. **102**, 702 (1995).
[8] A. E. Bennett, J. H. Ok, R. G. Griffin, and S. Vega, J. Chem. Phys. **96**, 8624 (1992); J. H. Ok, R. G. S. Spencer, A. E. Bennett, and R. G. Griffin, Chem. Phys. Lett. **197**, 389 (1992).
[9] D. K. Sodickson, M. H. Levitt, S. Vega, and R. G. Griffin, J. Chem. Phys. **98**, 6742 (1993).
[10] N. C. Nielsen, F. Creuzet, R. G. Griffin, and M. H. Levitt, J. Chem. Phys. **96**, 5668 (1992); R. Tycko and S. O. Smith, *ibid.* **98**, 932 (1993); Y. K. Lee, N. D. Kurur, M. Helmle, O. Johannessen, N. C. Nielsen, and M. H. Levitt, Chem. Phys. Lett. **242**, 304 (1995).
[11] N. C. Nielsen, H. Bildsøe, H. J. Jakobsen, and M. H. Levitt, J. Chem. Phys. **101**, 1805 (1994).
[12] D. P. Raleigh, F. Creuzet, K. Das Gupta, M. H. Levitt, and R. G. Griffin, J. Am. Chem. Soc. **111**, 4502 (1989); G. R. Marshall, D. D. Beusen, K. Kociolek, A. S. Redlinski, M. T. Leplawy, Y. Pan, and J. Schaefer, *ibid.* **112**, 963 (1990); A. E. McDermott, F. Creuzet, R. G. Griffin, L. E. Zawadzke, Q.-Z. Ye, and T. Walsh, Biochemistry **29**, 5767 (1990); F. Creuzet, A. McDermott, R. Gebhard, K. Van der Hoef, M. B. Spijker-Assink, J. Herzfeld, J. Lugtenburg, M. H. Levitt, and R. G. Griffin, Science **251**, 783 (1991); R. G. S. Spencer, K. J. Halverson, M. Auger, A. E. McDermott, R. G. Griffin, and P. T. Lansbury Jr., Biochemistry **30**, 10 382 (1991); A. M. Christensen, J. Schaefer, K. J. Kramer, T. D. Morgan, and T. L. Hopkins, J. Am. Chem. Soc. **113**, 6799 (1991); O. B. Peersen, S. Yoshimura, H. Hojo, S. Aimoto, and S. O. Smith, *ibid.* **114**, 4332 (1992); K. V. Lakshmi, M. Auger, J. Raap, J. Lugtenburg, R. G. Griffin, and J. Herzfeld, *ibid.* **115**, 8515 (1993); L. M. McDowell, S. M. Holl, S.-J. Qian, E. Li, and J. Schaefer, Biochemistry **32**, 4560 (1993); T. S. Balaban, A. R. Holzwarth, K. Schaffner, G.-J. Boender, and H. J. M. de Groot, *ibid.* **34**, 15 259 (1995).
[13] L. K. Thompson, A. E. McDermott, J. Raap, C. M. van der Wielen, J. Lugtenburg, J. Herzfeld, and R. G. Griffin, Biochemistry **31**, 7931 (1992); A. E. McDermott, F. Creuzet, R. Gebhard, K. Van der Hoef, M. H. Levitt, J. Herzfeld, J. Lugtenburg, and R. G. Griffin, *ibid.* **33**, 6129 (1994).
[14] H. Geen, J. J. Titman, J. Gottwald, and H. W. Spiess, Chem. Phys. Lett. **227**, 79 (1994); J. Magn. Reson. A **114**, 264 (1995).
[15] A. Schmidt and S. Vega, J. Chem. Phys. **96**, 2655 (1992).
[16] T. Nakai and C. A. McDowell, J. Chem. Phys. **96**, 3452 (1992).
[17] M. Mehring, in *Principles of High Resolution NMR in Solids*, 2nd ed. (Springer, New York, 1983).
[18] W. S. Veeman, Prog. NMR Spectrosc. **16**, 193 (1984); M. T. Duncan, in *A Compilation of Chemical Shielding Anisotropies* (Farragut, Madison, 1990).
[19] M. Wada, M. Sakurai, Y. Inoue, Y. Tamura, and Y. Watanabe, J. Am.

Chem. Soc. **116**, 1537 (1994); A. C. de Dios and E. Oldfield, *ibid*. **116**, 5307 (1994).
[20] P. Robyr, B. H. Meier, P. Fischer, and R. R. Ernst, J. Am. Chem. Soc. **116**, 5315 (1994).
[21] H. van Willigen, R. G. Griffin, and R. A. Haberkorn, J. Chem. Phys. **67**, 5855 (1977); R. A. Haberkorn, R. E. Stark, H. van Willigen, and R. G. Griffin, J. Am. Chem. Soc. **103**, 2534 (1981).
[22] W. P. Power and R. E. Wasylishen, Annu. Rep. NMR Spectrosc. **23**, 1 (1991); T. Nakai and C. A. McDowell, J. Am. Chem. Soc. **116**, 6373 (1994).
[23] T. Nakai and C. A. McDowell, Mol. Phys. **77**, 569 (1992).
[24] H. J. Simpson Jr. and R. E. Marsh, Acta Crystallogr. **20**, 550 (1966).
[25] M. S. Lehmann, T. F. Koetzle, and W. C. Hamilton, J. Am. Chem. Soc. **94**, 2657 (1972).
[26] A. Naito, S. Ganapathy, K. Akasaka, and C. A. McDowell, J. Chem. Phys. **74**, 3190 (1981).
[27] H. W. Spiess, in *NMR Basic Principles and Progress*, edited by P. Diehl, E. Fluck, and E. Kosfeld (Springer, Berlin, 1978).
[28] F. James and M. Ross, Minuit Computer Code, Program D-506, CERN, Geneva, 1977; Comp. Phys. Commun. **10**, 343 (1975).
[29] W. H. Press, B. P. Flannery, S. A. Teukolsky, and W. T. Vetterling, in *Numerical Recipes* (Cambridge University Press, Cambridge, 1986).
[30] Z. Gan, D. M. Grant, and R. R. Ernst, Chem. Phys. Lett. **254**, 349 (1996).
[31] M. E. Stoll, R. W. Vaughan, R. B. Saillant, and T. Cole, J. Chem. Phys. **61**, 2896 (1974).
[32] A. Naito, S. Ganapathy, and C. A. McDowell, J. Chem. Phys. **74**, 5393 (1981).
[33] H. J. Jakobsen, P. Daugaard, and V. Langer, J. Magn. Reson. **76**, 162 (1988).
[34] N. C. Nielsen, H. Bildsøe, and H. J. Jakobsen, J. Magn. Reson. **98**, 665 (1992); F. H. Larsen, P. Daugaard, H. J. Jakobsen, and N. C. Nielsen, J. Magn. Reson. A **115**, 283 (1995).
[35] H. J. Jakobsen, J. Skibsted, H. Bildsøe, and N. C. Nielsen, J. Magn. Reson. **85**, 173 (1989).
[36] S. K. Zaremba, Ann. Mater. Appl. **73**, 293 (1966); J. Conroy, J. Chem. Phys. **47**, 5307 (1967); V. B. Cheng, H. H. Suzukawa, Jr., and M. Wolfsberg, *ibid*. **59**, 3992 (1973).
[37] W. Zhu, C. A. Klug, and J. Schaefer, J. Magn. Reson. B **121**, 121 (1994).